



HAL
open science

New experimental approach for intelligent screening of buried metal/oxide/polymer interfaces via local electrochemistry: example of undamaged model epoxy-coated Zn alloys

Thomas Sanchez, Simon Gillet, Viacheslav Shkirskiy, Vincent Vivier, Jaques Echouard, Jolanta Światowska, Polina Volovitch

► To cite this version:

Thomas Sanchez, Simon Gillet, Viacheslav Shkirskiy, Vincent Vivier, Jaques Echouard, et al.. New experimental approach for intelligent screening of buried metal/oxide/polymer interfaces via local electrochemistry: example of undamaged model epoxy-coated Zn alloys. *Electrochimica Acta*, 2021, 367, pp.137411. 10.1016/j.electacta.2020.137411 . hal-02997685

HAL Id: hal-02997685

<https://hal.sorbonne-universite.fr/hal-02997685v1>

Submitted on 3 Dec 2020

HAL is a multi-disciplinary open access archive for the deposit and dissemination of scientific research documents, whether they are published or not. The documents may come from teaching and research institutions in France or abroad, or from public or private research centers.

L'archive ouverte pluridisciplinaire **HAL**, est destinée au dépôt et à la diffusion de documents scientifiques de niveau recherche, publiés ou non, émanant des établissements d'enseignement et de recherche français ou étrangers, des laboratoires publics ou privés.

1 ***New experimental approach for intelligent screening of buried***
2 ***metal/oxide/polymer interfaces via local electrochemistry: example of***
3 ***undamaged model epoxy-coated Zn alloys***

4
5 Thomas Sanchez¹, Simon Gillet¹, Viacheslav Shkirskiy¹, Vincent Vivier², Jaques Echouard³, Jolanta
6 Światowska¹, Polina Volovitch^{1*}

7
8 ¹ Chimie ParisTech - CNRS, PSL University, Institut de Recherche de Chimie Paris,
9 11 rue Pierre et Marie Curie, 75005 Paris, France

10 ² Sorbonne Université, CNRS, Laboratoire Interfaces et Systèmes Electrochimiques (LISE), 4 place
11 Jussieu, 75005 Paris, France

12 ³ Safran Landing Systems, Etablissement de Bidos – BP39, 64401 Oloron Sainte Marie Cedex
13 France

14
15 **Abstract**

16 A new simple experimental approach is proposed for *in situ* mechanistic studies of the underpaint
17 stability of metal/oxide/polymer interface under immersion. It allows an intelligent screening and fast
18 ranking of conversion coatings on Zn alloys designed for further application of organic coatings. The
19 approach is based on the application of a simple electrochemical aging protocol to the samples preliminary
20 coated with a model epoxy-polymer. The latter is enough thin to allow local electrochemical impedance
21 measurement and stable under this protocol, as revealed by attenuated total reflectance infrared
22 spectroscopy (ATR-IR) and electrochemical impedance spectroscopy (EIS). The interface stability and
23 degradation modes characterization is accessed via combined EIS, local electrochemical impedance
24 spectroscopy and mapping (LEIS and LEIM) and *in situ* optical imaging.

25 The developed approach allowed to discriminate two Zn alloy substrates, one with intact and another
26 with slightly damaged Cr(III) conversion layer, for which no strong differences in the electrochemical
27 behavior or average surface composition was visible prior to the epoxy-polymer application. The relative
28 stability of two substrates with model thin coating, evaluated in the developed electrochemical test,
29 correlated with the observations obtained for the same substrates coated with thick commercial epoxy
30 primer after 1000 h of immersion. The proposed methodology offers the possibility of a rapid intelligent
31 screening of various formulations of Cr(III)-based surface treatments for Zn based substrates designed for
32 paint applications.

33
34 **Keywords**

35 Local electrochemical impedance mapping (LEIM); Underpaint degradation; Zn alloys; conversion
36 coatings; AC-DC-AC

1
2
3
4
5
6
7

Highlights

- New approach for smart screening of conversion coatings is proposed
- Modified AC-DC-AC ageing procedure and model polymer are used
- Heterogeneous degradation of buried interfaces detected by LEIM and in situ imaging
- Relative stability in the new procedure correlates with immersion test

1. Introduction

Polymer coatings have been used for centuries for corrosion protection of metals and alloys due to their good barrier properties limiting water and oxygen access to the metallic substrates [1,2]. Barrier protection mechanisms of organic coatings have been extensively studied and the formulations of hydrophobic binders, as well as the addition of pigments, have been optimized to reduce the permeability of the coating to water and oxygen [3]. However, as water reaches the interface, underpaint reactivity can develop. Localized reactive spots under the polymer coating lead to the metal/oxide/polymer interface disbondment and delamination of the polymer coating from the metallic substrate. This delamination of the coating can accelerate the system degradation and must be considered with caution [4,5].

In order to ensure a good adherence of the polymer and improve corrosion resistance, the metallic interface is usually modified by conversion coatings [6]. These coatings are thin oxidized layers formed via chemical and/or electrochemical process at the metal surface [7,8,9]. Among conversion coatings, the most used in the last decades were chromate-based conversion coatings [10]. Their efficiency is supposed to be due to the combination of excellent anti-corrosion properties guaranteed by self-healing ability and good adhesion of chromates to polymer coating [11-12]. However, chromates were proved to be genotoxic and carcinogen [13] and since 2006, European legislation tries to tackle hexavalent chromium via Registration, Evaluation, Authorization and Restriction of Chemicals (REACH) and Restriction of the use of certain Hazardous Substances (RoHS) [14]. According to these legislations, the application of Cr(VI) compounds should be banned in Europe by 2022 even though some industries got several years of extension to find replacement solutions. Therefore, the development and the optimization of new chromate-free conversion coating is strongly required [15-16,17], whereas Cr(III)-based conversion coatings have been considered as a possible replacement [18,19].

In order to optimize the new generation of conversion coatings in a reasonable time scale, and to better understand their performances, it is necessary to develop new analytical tools to access the metal/oxide/polymer interface stability. To detect and localize the interfacial disbondment or deterioration, Scanning Kelvin Probe (SKP) is the most well-known and precise tool, used for both, blisters or delamination front detection and the measurement of the kinetics of polymer delamination front propagation in atmospheric corrosion [20,21]. SKP showed that delamination of a polymer with weak adhesion to zinc is mainly cathodically driven [22]. In immersion conditions, electrochemical impedance spectroscopy (EIS) is the most used technique to detect interfacial disbondment from an artificially introduced defect as well as to monitor the polymer coating degradation [23,24,25]. Different approaches have been developed to quantify the global degradation phenomena in painted systems: water uptake, diffusion of soluble ions, evolution of the total delaminated area etc. [26,27,28]. To localize the disbondment at polymer-metal interface, Local Electrochemical Impedance Mapping (LEIM) [29,30] and Scanning Vibrating Electrode (SVET) [31] can both detect the electrochemical reactivity in delaminated areas and distinguish the anodic and the cathodic reactive zones. However, contrary to LEIM, SVET cannot detect the underpaint reactivity in the absence of a defect in the paint. In addition, a quantitative LEIM was recently proposed to study the disbondment front propagation kinetics [32] during immersion. However, it should be mentioned that most of previously reported studies on local degradation of

1 metal/oxide/polymer interfaces using local electrochemical techniques concerned the interface
2 delamination starting from an artificial defect, intentionally introduced at the metal/oxide/polymer
3 interface or in the coating prior to the aging process.

4
5 For an undamaged coated surface, in addition to long term immersion, AC-DC-AC accelerated
6 electrochemical degradation procedure via alternating cathodic polarization (DC) and EIS measurement at
7 open circuit potential (AC) [33] is often used. Depending on the potential of the cathodic polarization
8 during AC-DC-AC procedure, it can either be used to assess the polymer stability [34,35], or to study the
9 underpaint reactivity and delamination [36]. The application of cathodic potential promotes the initiation
10 and propagation of the metal/oxide/polymer interface degradation [37]. Under polarization lower than -
11 1 V/SHE, both the oxygen reduction (**Eq. 1**) and the water reduction (**Eq. 2**) can occur [38] thus leading to
12 a pH increase at the buried metal/oxide/polymer interface. Using pH sensitive indicator like
13 phenolphthalein, these cathodic reactive areas can be evidenced by *in situ* Time Lapse Microscopy (TLM)
14 of the sample surface [39,40].



18
19 In the case of large cathodic over-potentials, high local pH, peroxides and free radicals can also damage
20 the polymer matrix; the polarization conditions should then be chosen carefully for each system and
21 should take into account the chemistry of the organic coating.

22 Epoxy resins are among the most used primers for Zn alloys because of their hydrophobicity and their
23 ability to incorporate fillers and pigments for corrosion inhibition, anti-fouling, self-healing, etc. [41]. Due
24 to the high impedance of thick commercial epoxy coatings and the presence of numerous additives, *in situ*
25 study of the underpaint reactivity in such a system by means of electrochemical tests, vibrational
26 spectroscopy and/or optical microscopy is often difficult and the results interpretation can be
27 controversial. In order to understand the underpaint reactivity, the use of a model polymer seems to be a
28 promising approach [42]. In the literature, several weakly adherent coatings, like polyvinyl butyral (PVB)
29 or polyvinyl alcohol (PVA), were used in SKP studies of underpaint reactivity [43,44]. However, they do not
30 sustain long term immersion because of their high solubility in water and weak adhesion to metallic
31 substrates [45]. For stability evaluations in long immersion and aggressive aging tests, some groups
32 performed experiment using thick epoxy polymers [29, 46]. Nonetheless, the measurements were either
33 made in atmospheric conditions or required to introduce a well localized artificial defect in the coating or
34 at the interface prior to the degradation procedures. The latter can influence the degradation mechanisms
35 and is not appropriate if the initial degradation is of interest.

36 Electrochemical impedance studies demonstrated that polymer also degrades in electrochemical
37 tests (see for instance [47,48]); however, to our knowledge, a combined approach, taking into account the
38 possible evolution of all the components of metal/oxide/polymer interfaces is still missing. It seems hence
39 to be timely to develop an experimental approach able to consider the initiation and propagation of the
40 underpaint reactivity and dissociate the intrinsic interface response from the possible polymer evolution
41 under electrochemical testing of buried metal/oxide/polymer interface. The later requires the
42 development of a model thin epoxy coating with a good adhesion to metal interfaces and characterized

1 stability [49],[50]. The model polymer should be homogeneous in terms of chemical composition and
2 thickness, thin enough for *in situ* electrochemical impedance measurements, transparent in the visible
3 light for an optical survey of the substrate/polymer interface and be stable to sustain AC-DC-AC procedure.
4

5 In this work, a new methodological approach is proposed for *in situ* accelerated mechanistic study of
6 the underpaint stability of zinc alloy/epoxy interfaces in immersion condition without introducing an initial
7 defect in the coated system. The methodology includes a specific aging procedure to accelerate the
8 interface degradation and the use of an optimized model epoxy polymer, meeting the requirements listed
9 above. The validation is made for a zinc alloy with Cr(III) conversion coatings designed for epoxy painting.
10

11 **2. Materials and methods**

12 **2.1. Materials**

13 **2.1.1. Substrates preparation**

14 Two substrate materials were used: hot dip galvanized zinc and zinc alloy coated steel.

15 Zn coated (hot dip galvanized, 0.2 wt. % of Al in the coating) plates of low carbon steel were used to
16 test the developed epoxy coatings, because the behavior of this material is well known and the response
17 of the epoxy can be easily distinguished from the response of Zn substrate. Prior to the application of
18 organic coating, the Zn samples were rinsed with Milli-Q water and degreased in 1 M NaOH solution for
19 30 s to remove the oxide layer and then rinsed with Milli-Q water and absolute ethanol before being dried
20 with compressed air.

21 Zinc-nickel alloy coating was used as the substrate for the conversion coating study. The alloy was
22 prepared by a following procedure. Steel plates of 10×15 cm² were degreased and grit-blasted.
23 Electrodeposition of Zn alloy was performed in alkaline 12-16 % ZnNi bath for 45 minutes at applied current
24 of 3 A/dm². After electrodeposition, the samples were rinsed with deionized water for 10 min and dipped
25 in trivalent chromium passivation bath, then rinsed for 3 min in deionized water and dried with
26 compressed air. Relief-baking of the samples was performed at around 200 °C for 23 h to alleviate
27 hydrogen embrittlement. X-ray fluorescence (XRF) measurement was performed by Fisherscope X-Ray
28 XDAL and showed 18 ± 2 μm in thickness and 14 ± 2 % in nickel composition. X-ray diffraction (XRD)
29 measurement was performed by Empyrean Panalytical and showed only the presence of the gamma phase
30 (Zn₁₁Ni₂). The Cr(III) content at the top surface was found to be between 5 and 9 at. % from the XPS
31 measurement.

32 In order to reduce adhesion of polymer coating to the substrate, conversion coating was modified for
33 some samples. For this, the samples of Zn alloy with conversion coating were immersed in 0.1 M NaOH for
34 5 s then rinsed with milli-Q water and dried with compressed air before application of polymer coating. Zn
35 alloy samples with modified conversion coating are referred as “samples of type 1” while the Zn samples
36 with non-modified conversion coating are referred as “sample of type 2” below. XPS characterization of
37 the surface could not evidence a chemical composition difference between the two types of coating within
38 a 2 % accuracy, which is consistent with the accuracy of the XPS measurement on rough surfaces.

1 For the model epoxy coating and degradation tests, 5×5 cm² samples were cut from the central part
2 of each 15×10 cm² plate to prevent the edge effects that can be observed in electrodeposition process.
3 Prior to the polymer coating, the samples were stored in a desiccator.
4

5 2.1.2. Epoxy coating

6 The model epoxy formulation was a DiGlycidyl Ether of Bisphenol-A prepolymer and TriEthylene
7 TetrAmine hardener (DGEBA-TETA) used in (1:1) ratio. One should note that Bisphenol-A is currently listed
8 in the Candidate List of substances of very high concern, however in this work it is not proposed for
9 industrial application but for methodological demonstration. If the method is applied at large scale,
10 alternative epoxy coating could be formulated. For viscosity requirements, the preparation was diluted in
11 3 mL of ethanol (analytical grade) for 4 g of mixture. Prior to spin-coating procedure, the preparation was
12 placed in a hermetic beaker and mixed at 300 rpm for 20 minutes then left to stand for 15 minutes in order
13 to remove air bubbles.

14 Just before the coating application, the surface of the substrate was rinsed with absolute ethanol to
15 improve the surface's wettability. The polymer coating was deposited by spin coating process using a
16 POLOS SP15 spin-coater. Once the sample was placed and held in the spin-coater, the resin was poured in
17 large excess and spread on the whole surface, the spin coating was performed twice with a 15 s relaxation
18 time in between with following parameters: 3000 RPM rotary speed and 500 RPM/s linear acceleration for
19 35 s. After spin-coating, the samples were cured at 50 ± 5 °C for 14-16 h for curing and desolvation [51].

20 With this procedure, the obtained coating's thickness controlled by optical microscopy (see section
21 2.2.2. for details of optical measurement) was *ca.* 10 ± 1 μm.

22 The samples were stored in a desiccator between the coating application and the degradation test.
23 Degradation tests were made in the following week.

24 The chemical bonds formed after curing for stoichiometric formulation were reported in literature [52]
25 and are schematically presented in **Fig. 1** [53].

26 <Fig. 1>

27 For the tests eight 5×5 cm² samples of each type (type 1 and type 2 described in section 2.1) were
28 coated with model epoxy polymer and tested with the adapted AC-DC-AC procedure as detailed hereafter
29 (see section 2.3.2). For comparison, additional four samples (size 10×15 cm², two of each type) were also
30 coated with a 60 μm thick layer of a commercial epoxy primer paint. The last four samples were used in
31 1000 h immersion test and AC-DC-AC degradation tests. These panels are named hereafter as "industrial
32 epoxy coating". To distinguish the same substrates covered with two different coating, the letter A is
33 added to the name/type of the sample with the industrial thick epoxy coated samples and the letter B for
34 the samples with model epoxy. The combinations of studied substrates and coatings are summarized in

35 **Table 1.**

36 <Table 1>

2.2. Polymer characterization

No specific drying procedure was used before *ex situ* measurement except the electrolyte removal from the surface by compressed air. The evolution of the hydrophobic properties of the polymer were followed by static drop contact angle measurements using a Dataphysics OCA 15EC Package 2 contact angle automatic system with SCA 20 software module using a drop of 25 μL Quartex water deposited from 1 cm height. Each measurement was repeated 3 times with 3 drops and 3 different locations on each sample.

The chemical evolution of the polymer matrix was studied by Attenuated Total Reflectance Infrared Spectroscopy (ATR-IR) with Bruker Tensor 27 equipped with a Pyke MIRacle™ single reflection ATR. ATR was used in a standard configuration with the coating directly pushed against the crystal. Each IR spectrum was recorded from 4000 to 400 cm^{-1} with a resolution of 2 cm^{-1} and integrated over 512 cycles, at least two spectra were measured for each sample at two different locations. Before every ATR measurement, the crystal was cleaned with absolute ethanol and a background measurement was performed for the cleaned crystal. Before the measurement, a spectrum of a reference coated sample stored in a desiccator was recorded. Thus, the reproducibility of the measurement could be verified so that normalization of the IR spectra of degraded samples was unnecessary. This protocol was proposed since during degradation of the polymer coating no constant peak could be defined in the ATR-IR spectra. The peaks positions of the characteristic functional groups in DGEBA-TETA epoxy resin followed in this study [54,55] are presented in **Table 2**.

<Table 2>

Optical characterization of the samples was performed using a Keyence VHX-5000 3D microscope. Due to its short depth of focus ($< 1 \mu\text{m}$), it was possible to measure the thickness of the model epoxy by focusing alternatively on the non-coated substrate and on the top of the transparent coating using the reflection of the confocal light source. It was also used to observe the presence of corrosion products under the coating, as well as the deformation of the top surface of the coating in 3D-composition mode.

2.3. Degradation procedures

Three different degradation procedures were used. One sample was also kept in a desiccator after curing to obtain the evolution of a reference coating.

1. A humid chamber was used the first stability verifications of the model epoxy. Two samples were kept above 90 % relative humidity at room temperature. For contact angle and ATR-IR measurements, every hour they were taken out, rinsed with Milli-Q water and dried with compressed air before placed back in the humid chamber.

2. An immersion was used to verify immersion stability of the model epoxy. Four samples were immersed in 25 mL solution of 0.01 M NaCl with 1 wt. % of phenolphthalein in a sealed glass cell of 4.4 cm in diameter at room temperature. According to the literature, the influence of the phenolphthalein on the cathodic reactivity of polymer/zinc alloy interface can be neglected³². To perform *ex situ* measurements during immersion, samples were rinsed with milli-Q water and dried with compressed air before measurements and placed back to the immersion solution in less than 5 min. Immersion electrolyte was

1 kept in a beaker during *ex situ* characterization and poured into the electrochemical cell to continue
2 immersion test.

3 **3.** An AC-DC-AC test was applied to study the metal/oxide/polymer interface stability. For this test an
4 electrochemical cathodic polarization cycling was performed on 5 coated samples. The samples were
5 immersed for 1 hour in 25 mL of 0.01 M NaCl with 1 wt. % of phenolphthalein at room temperature to
6 reach a stable value of open circuit potential (OCP). After the first EIS measurement, AC-DC-AC cycling was
7 performed as presented in **Fig. 2**. It consisted of 15 minutes of cathodic polarization at -1.5 V/Ag/AgCl
8 followed by 15 min immersion at OCP and a remaining period of 30 min for different measurements at the
9 OCP. The procedure lasted 7 cycles for a total duration of 8.5 hours. After the cycling and before *ex situ*
10 characterizations the sample was rinsed with milli-Q water and dried with compressed air.

11 <Fig.2>
12

13 **2.4. Electrochemical characterization and Time Lapse Microscopy**

14 Electrochemical impedance spectroscopy (EIS) was performed using a Solartron Modulab potentiostat
15 with ECS software interface. The three-electrode electrochemical cell consisted of a silver/silver-chloride
16 (Ag/AgCl) reference electrode (RE), a 6.6 mm in diameter graphite rod as counter electrode (CE) and the
17 coated sample as working electrode (WE). The cell was placed in a Faraday cage to avoid external
18 interferences. EIS spectra were carried out at the OCP from 100 kHz to 0.1 Hz with 6 points per frequency
19 decade and 10 mV_{RMS} sinewave signal. Evolution of the low frequency (0.1 Hz) impedance modulus was
20 used for tracking the stability of the metal/oxide/polymer interface.

21 Separately, local electrochemical impedance mapping (LEIM) was performed on three additional
22 samples under AC-DC-AC tests. The electrochemical setup is described in detail in [30]. The local probe
23 consisted of two Ag wires of 150 μm in diameter sealed in twin-capillaries using 3M glue. The distance
24 between the two wires was 400 μm . The capillaries were bended so that the Ag electrodes were
25 perpendicular to the surface of the sample, and thus, only the normal contribution of the current density
26 was monitored. AgCl was deposited on both Ag electrodes of the probe prior to LEIS experiment by 5 min
27 potentiostatic oxidation at 0.4 V/Ag/AgCl in 0.5 M NaCl solution. OCP and EIS measurements of the
28 Ag/AgCl surfaces of the probe were performed during its immersion in 0.01 M NaCl solution at different
29 times between 5 min and 10 h after the preparation of the probe to verify its stability. A home-made setup
30 using Solartron Modulab software with auxiliary input and a 3-axis stepper motor-controlled by Sensolytics
31 was used for LEIM measurements. The working electrode was a 2 cm diameter sample's surface. The
32 counter electrode was a 3 cm diameter toroid of platinum wire placed above the surface of working
33 electrode to guarantee symmetrical distribution of the current lines. During the measurement, the probe
34 to sample distance was fixed at $100 \pm 25 \mu\text{m}$. For electrochemical impedance mapping, the potential
35 oscillation was set to 15 mV_{RMS} and 100 Hz; the X-Y maps consisted of a square grid of 31 \times 31 points distant
36 of 100 μm to cover a 3 \times 3 mm² area, the mapping was performed in 18 min.

37 *In situ* time lapse microscopy (TLM) using an HD USB microscope with 2 MP CMOS detector and a 4000
38 K white LED enlightenment was set up in the electrochemical cells for both AC-DC-AC and local
39 electrochemistry tests. The objective to surface distance was set to 4 cm for a magnification of $\times 80$, leading
40 to a 100 μm^2 pixel size. A picture was taken every minute during immersion. Local underpaint cathodic

1 reactivity was detected from the color change of phenolphthalein, turning from colorless to pink color in
2 the pH range of 8.2 - 10. The increase of pH due to cathodic OH⁻ release (reactions 1-2) is relevant for both,
3 immersion and cathodic polarization. Percolation of the polymer and opening of pores could also be
4 observed by TLM during immersion test. During cathodic polarization in the AC-DC-AC test, the localized
5 hydrogen evolution can be monitored.

6 The experiments were made in a closed system in order to limit evaporation and keep constant
7 electrolyte level (marked in the cell). This was achieved with the use of parafilm grafting tape, sealing the
8 electrochemical cell and the parts of the setup (objective etc.). The electrolyte level visually stayed
9 constant during 7.5 hours of the testing procedure.

10 Degradation procedures and characterizations used for the evaluation of the samples of different
11 types are listed in **Table 1**.

13 3. Results

14 3.1. Stability of the epoxy coating on Zn substrate during immersion

15 **Fig. 3.a** shows typical ATR-IR spectra of the epoxy coated Zn samples at different times of immersion.
16 The peaks attribution is shown in **Table 2**. The peaks referred as 6 and 1 correspond to characteristic peaks
17 of OH⁻ groups for scissors and stretching vibrations. The scissors vibration at 1644 cm⁻¹ is related to the
18 water molecule and is referred as “free OH” while the stretching vibration at 3400 cm⁻¹ is related to all the
19 OH groups and is referred as “total OH” [56,57]. The evolution of the peak’s intensities averaged for the
20 four immersed samples and the standard deviation are presented in **Fig. 3.c**. Both intensities increase and
21 follow the same exponential trend (**Eq. (3)**) for the first 65 h. This trend is consistent with the water uptake
22 of the coating, which seems to reach the saturation level from 20 to 25 hours of immersion: both peaks
23 intensities associated with OH become stable. After 65 to 77 h of immersion, the intensities of these peaks
24 change suddenly: the peak 1 corresponding to the “total OH” increases, whereas the peak 6 associated
25 with the “free OH” decreases. This change in intensity is attributed to chemical evolution within the epoxy
26 polymer coating occurring at around 70 h of immersion in a 0.01 M NaCl solution. The experimentally
27 observed evolution of the OH-group peaks intensities with time could be fitted with the empirical equation
28 (3) for both OH peaks.

$$29 \quad A(t) = A_{\text{sat}} - A_1 \times e^{-b \times t} , \quad (3)$$

30 In equation (3), t is the immersion time, $A(t)$ is the peak intensity at time t , A_{sat} is the peak intensity
31 at saturation, A_1 is the pre-exponential factor, and b is the exponential time constant obtained from the
32 fitting. The value $b = 0.16 \pm 0.01 \text{ s}^{-1}$ was the same for both “free OH” and “total OH” peaks evolution.

33
34 **Fig. 3.d** shows the average evolution of the intensities of the peaks attributed to the typical organic
35 bonds in DGEBA-TETA epoxy coating 2, 3, 4 and 5 in **Table 2** for the four samples during immersion. For
36 clarity, standard deviation of the measurement is not shown in the figure; however, the tendency was
37 similar for all four samples. Their intensities are stable for the first 60 hours of immersion; therefore, it can
38 be considered that only water uptake occurred during this period. After 60 hours, all the peaks’ intensities
39 attributed to the typical organic bonds in epoxy matrix (see **Table 2**) decrease strongly. This intensity drop
40 coincides with the change in behavior of the two peaks corresponding to OH positions. These trends

1 confirm that the model DGEBA-TETA epoxy coating starts to degrade after around 70 hours of immersion
2 in a 0.01 M NaCl solution at room temperature.

3 <Fig. 3>

4 In addition to ATR-IR spectra, the evolution of the contact angle is shown in **Fig. 4.a**. The contact angle
5 of the reference sample stored in humid air was also measured for comparison. Under both conditions,
6 immersion and humid air, the contact angle drops from 75° to around 70° during the first hour that
7 evidences a first decrease in hydrophobicity. This can be attributed to the hydration of the top surface of
8 the epoxy coating. Until the 70th hour, the contact angle remains stable (70° for all samples). After 70 hours
9 of immersion, the contact angle decreases down to 60° and the values become more scattered depending
10 on the analyzed areas. The increase in hydrophilicity of the coating corroborates with ATR-IR results: a first
11 phase of water accumulation within the firsts hours, a saturation of water and stability domain of the
12 system up to 50 hours and after 60-70 hours, the beginning of model epoxy matrix degradation.

13 <Fig.4>

14 *In situ* optical TLM images (**Fig. 5 a**) show no change of the surface up to 50 hours of immersion.
15 Between 50 and 75 hours of immersion (**Figs. 5b, d, and e**) localized porosity appears and formation of
16 corrosion products becomes visible around some open pores. A sudden formation of corrosion products
17 with the opening pores could indicate the onset of Zn dissolution under the coating prior to the coating
18 degradation and the decrease in the cross linking. This initial underpaint reactivity can be possible due to
19 porosity of the polymer coating. **Fig. 5.c and f** show the coating analysis in 3D microscope after 10 hours
20 and 75 hours of immersion consequently. The images are reconstructed using a high-resolution 3D-
21 composition over 20 optical images taken over 9 μm depth range. The colors are attributed to light
22 reflection, thus corresponding to the deformation of the coating due to the growth of corrosion products
23 underneath the coating or by swelling. It can be seen that the coating surface is significantly deformed
24 after the immersion test (**Fig. 5.c**) if compared to non-deformed state (**Fig. 5. f**), which can be attributed
25 to the swelling of the polymer and also is coherent with the ATR IR observed water content increase. The
26 coating deformation is measured to be *ca.* 8 μm protruding above the initial coating surface.

27 <Fig. 5>

28 Typical electrochemical impedance spectra of the Zn coated samples after 1 and 72 hours of
29 immersion are presented in **Fig. 6.a**. The EIS spectrum after 1 h of immersion shows two separate
30 depressed semi-circles attributed to the polymer coating in the high frequency domain (1000 – 5 Hz) and
31 the double layer at the metallic interface in the lower frequency domain (5-0.1 Hz) as reported in
32 literature²⁴. After 1 h of immersion the presence of second semi-arc at low frequencies clearly shows the
33 existence of a double layer capacitance with a value of *ca.* 1 μF cm⁻². It clearly indicates that the polymer
34 coating is highly porous so that water can reach the metallic substrate during this period of immersion.
35 Moreover, it evidences also that the metallic surface is not entirely covered by the model epoxy coating,
36 i.e. there are some zones with pre-existing disbondment at the metal/oxide/polymer coating interface.
37 The Nyquist plot after 72 hours of immersion shows a single depressed semi-circle attributed to the
38 response of the delaminated metallic surface. However, the contribution from the polymer coating and
39 and the corrosion product layer cannot be completely excluded at this time. A thorough data analysis with
40 the fitting was attempted but no simple equivalent circuit was found to fit correctly this single time
41 constant. Various parameter combinations could give valid fitting without proper physical meaning.

1 The evolution of the electrochemical impedance modulus at 0.1 Hz during the immersion is presented
2 in **Fig. 6.b**. The impedance value of *ca.* 30 kΩ cm² remains stable with an abrupt drop at 50 hours to a
3 steady value of *ca.* 5 kΩ cm². The decrease of electrochemical impedance modulus can be explained as a
4 loss of adherence and the degradation at the paint/metal interface due to the formation of pores in the
5 coating. It should be noted that the polymer composition remains stable during 50 hours as confirmed
6 from ATR-IR and TLM observations (*vide supra*).

7 <Fig. 6>

8 **3.2. Stability of the epoxy coating on Zn substrate under AC-DC-AC cycling**

9 In order to prove the applicability of the proposed model epoxy coating for a fast-electrochemical
10 assessment of epoxy paint/metal interface, the evolution of the model epoxy coating was surveyed during
11 the AC-DC-AC test.

12 The ATR-IR spectra on **Fig. 3.b** show no variation in the peak intensities related to the characteristic
13 groups of the epoxy matrix except the peak 5 corresponding to the C-H bond, while both peaks
14 corresponding to “free OH” and “total OH”, see **Table 2**, increase in intensity which is relevant to water
15 uptake. In addition, the hydrophobicity measured by contact angle remains stable throughout the 6
16 polarization cycles, as presented in **Fig. 4.b**. The results are coherent with water uptake in the polymer
17 pores without polymer degradation. As for the immersion test, electrochemical impedance at low
18 frequency, shown in **Fig. 6.c**, is also stable for 4 cycles and decreases after the 5th cycle.

19 It can be then concluded, that the proposed model epoxy coating can sustain up to 50 hours of
20 immersion or 7 cathodic polarization cycles without degradation. In addition, with both degradation
21 procedures, the polymer did not show any sign of degradation until the disbondment occurred at the
22 metal/oxide/polymer interface [58].

24 **3.3. Zn alloy/oxide/model epoxy interface evolution under modified AC-DC-AC test**

25 The developed epoxy coating was applied on the Zn alloy with two types of conversion coating defined
26 as described in the experimental part (section 2.1.1: damaged and undamaged samples corresponding to
27 sample 1 and sample 2, respectively). The modified AC-DC-AC procedure was used to compare the
28 electrochemical stability of zinc alloy/conversion coating/polymer interfaces in these two systems.

29 In the first step, the behavior of two types of samples without application of the polymer was
30 compared. After one hour of immersion in a 0.01 M NaCl solution, the OCP of both types of samples was
31 around -0.56 V vs. Ag/AgCl. Furthermore, the samples with both types of conversion coating show a similar
32 EIS response (**Fig. 7.a**). A slight difference in the roughness of the Zn alloy substrate can change the angle
33 in the CPE used for the fitting [59], and can explain the slight differences in the shape of the Nyquist plot.

34 <Fig. 7>

35 In contrast, once the samples are coated with the model epoxy coating (referred as type 1B and type
36 2B in **Table 1**), the electrochemical behavior of the two systems is quite different (**Fig. 7.b**). The steep
37 decrease in the low frequency electrochemical impedance modulus ($|Z|$ 0.1 Hz) from the 3rd cycle (**Fig.**
38 **7.c**) shows an important increase of the system reactivity in the case of the samples of type 1, while the

1 impedance modulus value remains almost the same for the samples of type 2 during all the 7 cycles. For
2 comparison, in the Zn samples without conversion coating (Fig. 6), the degradation of the
3 metal/oxide/polymer interface was visible from the sharp decrease of electrochemical impedance
4 modulus. Thus, the difference in the evolution of the EIS of Zn alloy with conversion coatings of type 1 and
5 2 (sample type 1B and 2B) with cycling reveals a lower adherence of the model paint to the substrate in
6 the case of type 1 samples than in the case of type 2 substrates.

7 The *in situ* microscopy images of both samples after 3 and 5 degradation cycles are presented in **Fig.**
8 **8**. The sample of type 1B (**Fig. 8 left**) shows a more significant cathodic hydrogen evolution (**Eq. 2**) than the
9 sample of type 2B as it can be evidenced by the bubbles present on the surface. In addition, the spreading
10 of pink-colored areas on the surface of type 1B sample indicates the presence of OH⁻ ions (**Eq. 1** and **Eq. 2**)
11 inside and over the coating because of the phenolphthalein indicator in the electrolyte. Although the
12 oxygen reduction reaction can occur during the modified AC-DC-AC degradation cycling for both types of
13 samples, no OH⁻ were detected by the indicator on the sample of type 2B (**Fig. 8 right**).

14 <Fig. 8>

15 Thus, *in situ* TLM confirms EIS results under modified AC-DC-AC procedure: samples of type 1 show a
16 much weaker bonding at the metal/oxide/polymer interface than the samples of type 2. The difference in
17 the surface properties of the sample type 1 and type 2 was not observed by EIS before epoxy coating
18 application, however the proposed AC-DC-AC procedure applied on the epoxy coated samples in
19 combination with EIS and TLM observations allowed easily to evidence a difference between these two
20 types of samples.

21 3.4. Spatial distribution of underpaint reactivity

22 **Fig. 9 a** presents an example of *in situ* image of a sample of type 1B, coated with the developed epoxy
23 coating. The picture was taken after the relaxation step of the 4th AC-DC-AC cycle, just before the LEIM
24 measurement. Localized hydrogen evolution as well as slightly pink areas corresponding to oxygen
25 reduction reaction sites are clearly visible in the figure. **Fig. 9 b** shows the LEIM map of the modulus of the
26 local electrochemical admittance, i.e. the inverse of impedance, recorded at the 3×3 mm² area delimited
27 by black square on the TLM image in **Fig. 9 a**. While TLM shows no visual degradation (no pores in the
28 polymer, no corrosion products, no pink color indicating high pH) until at least 3 cycles, LEIM clearly
29 demonstrates inhomogeneous distribution of the local admittance, revealing localized damage at the
30 metal/oxide/polymer interface. Indeed, the zones indicated by red color in **Fig. 9 b** have the values of
31 admittance about one order of magnitude higher compared with the other parts of the scanned surface.
32 The measured admittance values up to 0.5 2 μS cm⁻², meaning the current is in the mA range, ensure that
33 the developed epoxy coating allows a proper measurement of the underpaint reactivity. One should note
34 that even if Fig. 9 illustrates only one example of the zone with LEIM detected inhomogeneous reactivity,
35 strongly inhomogeneous degradation was detected in multiple locations for the samples of Type 1. For
36 comparison, in the same testing procedure, the samples of Type 2 did not show degradation neither by
37 TLM (**Fig. 8 b**) nor by LEIM (not shown).

38 <Fig. 9>

39 In order to verify that the interface evolution under the model thin epoxy polymer is coherent with
40 the degradation expected under a thick strong industrial epoxy polymer, and in order to verify if the

1 difference between the conversion coatings of type 1 and type 2 can be detected by LEIM under such a
2 thick layer, additional tests were made with the samples 1A and 2A, coated by industrial paint.

3 The samples of type 2A with thick coatings did not evolve neither in TLM nor in LEIM during 10 AC-DE-
4 AC cycles and are not shown in the figures. The samples of type 1A coated with the same industrial paint
5 formed blisters during cycling. **Fig. 9 c** shows a typical *in situ* TLM image of a sample of type 1, coated with
6 industrial epoxy coating after 10 AC-DC-AC cycles. Blisters are clearly visible on the surface, indicating
7 localized degradation of the metal/oxide/polymer interface in their vicinity. The black square on the TLM
8 image represents the 4×4 mm² area scanned by LEIM. The LEIM measured at 100 Hz is presented in **Fig. 9**
9 **d**. At the same time, the LEIM map shows a homogenous distribution of admittance values around 0.2 μS
10 cm⁻². Although the presence of degraded area on the sample detected by TLM, the high impedance of the
11 applied epoxy primer masks the electrochemical response from the metal/oxide/polymer interface in the
12 case of our small local impedance probe.

13 Finally, several samples of type 1A and 2A with industrial coating were immersed for 1000 hours in the
14 demineralized water. After the test, the samples of type 1A were blistered while the samples of type 2A
15 did not. To conclude, the LEIM experiments with model epoxy clearly distinguished two types of
16 conversion coatings, evidenced the localized character of degradation and gave the relative stability order
17 similar to the order obtained in immersion tests and AC-DC-AC tests of the same substrates coated by
18 industrial coating.

20 4. Discussion

21 4.1. Speculative degradation mechanism of model epoxy

22 Three steps of evolution were observed for the model zinc/epoxy interface with developed DGEBA-
23 TETA epoxy polymer exposed 0.01M NaCl electrolyte, as demonstrated by combined EIS, ATR-IR and
24 contact angle measurements:

- 25 - A saturation of the model epoxy coating by water reaching the metal/oxide/polymer interface during
26 the first hours;
- 27 - A stable behavior of the polymer coating until the polymer disbondment at the metal/oxide/polymer
28 interface at around 50 hours of immersion;
- 29 - A polymer coating degradation after 70 h of immersion.

30 *In situ* TLM demonstrated the emergence and the opening of pores, the percolation of the epoxy coating,
31 which can be attributed to a decrease of the cross-linking of the polymer. The evolution of the ATR-IR
32 peaks corresponding to characteristics bonds of epoxy polymer also evidences that the organic bonds were
33 most likely broken during the polymer's degradation (**Fig. 1.b**). Our results also demonstrated that the
34 degradation of both the metal/oxide/polymer interface and the epoxy coating was enhanced by the
35 cathodic polarization cycling of the coated samples. During AC-DC-AC aging procedure, hydroxides ions
36 were detected by TLM, which is in agreement with **Eq. 1**.

37 The degradation mechanism of the polymer coating seems hence to be driven by the local pH increase.
38 Consequently, with a stronger metal/oxide/polymer interfacial bonding the cathodic current under
39 polarization cycling would be reduced leading to a less significant increase of pH under the paint. Hence,

1 the developed model epoxy coating could sustain more severe AC-DC-AC degradation test, such as lower
2 potential or increased number of cycles, for the systems with optimized conversion coating.

3 Leached by the substrate anodic dissolution metallic cations or possible presence of intermediate
4 peroxides formed by the cathodic reactions reported in Refs. [60,61] could also accelerate polymer
5 degradation, however our work is not able to confirm or disclaim their production and their role in the
6 degradation mechanism.

8 **4.2. Applicability of the modified AC-DC-AC protocol to discriminate conversion coatings**

9 The combination of local electrochemical impedance and *in situ* Time Lapse Microscopy evidenced
10 that the methodology using DGEBA-TETA polymer coating and modified AC-DC-AC procedure permitted
11 to detect localized metal/oxide/polymer interface degradation. A speculative schema of the
12 metal/oxide/polymer interface degradation process induced by the test is presented in **Fig. 10**. Once water
13 and aggressive species diffuse through the polymer and reach the metal/polymer interface, deadhesion is
14 stronger for conversion coating of type 1 samples than for type 2 samples. More intensive cathodic
15 reaction leads to a quicker evolution of the impedance modulus with time for type 1 samples than for type
16 2 samples. Finally, hydroxides generated at the interface, diffuse through the coating and degrade the
17 polymer, which arrives quicker for the type 1 sample than for type 2 sample.

18 <Fig. 10>

19 The approach allowed to discriminate two conversion coatings on Zn alloys as a function of their ability
20 to form a stable metal/epoxy polymer interface. The proposed methodology is of great interest, because
21 the results can be obtained in approximately 24 hours (1 hour for the coating preparation, 14 hours for
22 curing, 9 hours for the measurements), in comparison to the commonly used 1000 hours of immersion.
23 Thus, this methodology can be used as a fast and smart screening test of conversion coatings on Zn alloys
24 for epoxy primers compatibility. In addition, it could give more comprehensive insights into the
25 degradation mechanism of the metal/oxide/polymer interface such as its sensitivity to cathodic
26 delamination. The combination of TLM and LEIM can indicate the heterogeneous or homogeneous nature
27 of the metal/oxide/polymer disbandment at different scales and with a spatial resolution of approximately
28 100 μm .

29 The proposed methodology evaluates the intrinsic stability of conversion coating in confined zones
30 under epoxy polymer and discriminates coating with close chemistry. Such an approach however cannot
31 take into account possible variations of conversion layer stability related to interactions between the
32 conversion coating and an industrial epoxy polymer, containing numerous additives. Comparison of
33 conversion coatings with very different chemistry and hence probably different degradation mechanisms
34 can be also erroneous without additional characterizations. Though, chemical characterization of the
35 interface and of the effect of the polymer chemistry on the stability of the conversion layer with several
36 model polymers could nicely complete the proposed approach.

4.3. Physical interpretation of LEIM on undamaged coated samples

Although LEIM is a common technique in the investigation of metal/oxide/polymer interface, most published studies demonstrate that pre-degraded polymer coating with either scarification and/or drilling of the coating was used to initiate the delamination process [29]. Other groups have studied blistering mechanism, i.e. a destabilization of buried metal/paint interface via LEIM without the generation of a localized defect in the coating. In most cases, the reactivity was enhanced at metal/oxide/polymer interface by using either NaCl salt powder or a drop of NaCl solution at the defined area of the metal substrate prior to the polymer coating deposition [62],[63]. Thus, in these experiments a detection of the defect was foreseen. In our work, in order to initiate the metal/oxide/polymer interface reactivity, the conversion coating was slightly degraded then the samples were cleaned prior to paint application so that the loss of stability of the buried metal/oxide/polymer interface was only originating from the conversion coating quality. According to our knowledge, this approach with the unknown random distribution of surface defects before measurements, corresponding to the potentially weak interfacial bonding, was used for the first time.

On the other hand, one could contest the accurate contribution of the underpaint reactivity detected by LEIM in this work. Indeed, this technique is often used to detect defects within the organic coating itself more than at the hidden metal/oxide/polymer interface [64]. One could then wonder whether the active sites detected by LEIM were related to interfacial reactivity or to intrinsic defects in the polymer like a localized higher porosity of the model coating [65] or locally thinner polymer [66] as described in the literature. Indeed, the existence of local high porosity in the polymer coating could induce a higher diffusion of oxygen under cathodic polarization and therefore, pH increase leading to the locally accelerated disbondment. A corollary hypothesis would be that these intrinsic defects in the polymer coating could result from the presence of a locally damaged conversion coating underneath: during the paint application and curing, the constraint relaxation within the polymer coating could lead to a segregation of intrinsic defects in the vicinity of a locally weaker metal/oxide/polymer interface. However, as described by Taylor *et al.* [65] the presence of underpaint reactivity and, therefore, the corrosion products in the pores leads to an enhancement of the barrier effect, thus, the increase of impedance modulus of the system. It was pointed out, that the deposition of zinc corrosion products occurs very shortly after the pore opening in the coating, indicating that the underpaint metal already reacts.

The question of the initiation of the local reactivity remains uncertain, both metal/oxide/polymer disbondment and intrinsic defect in the polymer could be the origin of the local reactivity, and might also be linked one to another. Still, this behavior was only evidenced on the samples of type 1, i.e. with supposedly weaker metal/oxide/polymer interface.

5. Conclusions

A new methodology using a model epoxy polymer and adapted to an AC-DC-AC accelerated degradation procedure was proposed to study and to understand stability of buried metal/oxide/polymer interface. It allowed to discriminate conversion coatings on zinc alloys in terms of ability to generate a stable metal/oxide/polymer interface in epoxy coated systems. The relative stability of two substrates with model thin coating, evaluated in the developed electrochemical test, correlated with the observations

1 obtained for the same substrates coated with thick commercial epoxy primer after 1000 h of immersion.
2 The proposed testing procedure lasts less than 24 h compared with a classical immersion test, making it
3 interesting for the fast and smart ranking of the quality of conversion coatings.

4 In addition, the combination of in situ optical imaging and local electrochemical impedance in the
5 accelerated test allowed to identify the heterogeneous character of interfacial disbondment on a large
6 surface for which the possible locations from which the degradation can initiate are initially unknown and
7 randomly distributed. This allows to obtain reliable results without preliminary introducing of an artificial
8 defect as usually reported in the literature. The latter allows to have the true response of the sample
9 protected by the coating without having to ask the question of the driving role that the artificial defect
10 could have on the degradation of the coating.

11

1 References

- [1] T. Prosek, *Mechanisms of degradation of organic coatings*, The Journal of Association of Corrosion Engineers 61 (2017), 155-161
- [2] G. W. Walter, A critical review of the protection of metals by paints, *Corrosion Science* 26 (1986), 27-38
- [3] M. F. Montermor, Functional and smart coatings for corrosion protection: A review of recent advances, *Surface and Coatings Technology* 258 (2014), 17-37
- [4] W. Funke, Towards environmentally acceptable corrosion protection by organic coating, *Anti Corrosion* (1984), 4-7
- [5] W. Funke, Problems and progress in organic coatings science and technology, *Progress in Organic Coatings* 31 (1997), 5-9
- [6] W. Funke, The role of adhesion in corrosion protection by organic coatings, *Journal of the oil and colour chemists' association* 68 (1985), 229-232
- [7] G. L. Song, *Surface Engineering of light alloys* (2010), 3-39
- [8] A.S.H. Makhlof, Current and advanced coating technologies for industrial applications, *Nanocoatings and Ultra-Thin Films* (2011), 3-23
- [9] T. Biestek, J. Weber, Electrolytic and chemical conversion coatings: a concise survey of their production, properties and testing, *J. Electrolytic and Chemical Conversion Coatings* (1976), 200
- [10] J. Zhao, R.L. McCreery, G.S. Frankel, *Effects of chromate and chromate conversion coatings on corrosion of aluminum alloy 2024-T3*, *Surface and coating technologies* 140 (2001), 51-57
- [11] D. Gilroy, P.J. Eddowes, , F.L. Bentes, *Techniques for assessing the protective properties of chromated conversion coatings—Part II: Galvanized steel*, *Metal Finishing* 94 (1996), 14-22
- [12] C.S. Jeffcoate, H.S. Isaacs, A.J. Aldykiewicz, M.P. Ryan, Chromate in conversion coatings: a XANES study of its concentration and mobility, *JACS* 122 (2000), 540-547
- [13] U.S. EPA (1998) Principles of Environmental Impact Assessment Review: Appendix A: Environmental Impact Assessment Checklist
- [14] European Commission regulation report n°2017/999 - REACH, Official Journal of European Union (2017)
- [15] G.D. Wilcox, J.A. Wharton, *A review of chromate-free passivation treatments for zinc and zinc alloys*, *Transactions of the Institute of Metal Finishing* 75 (1997), B140-B142
- [16] G. Wilcox, *Replacing chromates for the passivation of zinc surfaces*, *Transactions of the Institute of Metal Finishing* 81 (2003)
- [17] J.W. Bibber, Non-chrome-containing conversion coatings for zinc and zinc alloys: Environmentally friendly alternatives provide equal or better adhesion and corrosion resistance as conventional methods, *Metal Finishing* (2008), 41-46
- [18] R. Berger, U. Bexell, T.M. Grehk, S.E. Hörnstörm, A comparative study of the corrosion protective properties of chromium and chromium free passivation methods, *Surface and Coating technologies* 202 (2007), 391-397
- [19] X. Zhang, C. van den Bos, W.G. Sloof, A. Hovestad, H. Terryn, J.H.W. de Wit, *Comparison of the morphology and corrosion performance of Cr(VI)- and Cr(III)-based conversion coatings on zinc*, *Surface and Coating Technologies* 1999 (2005), 92-104
- [20] A. Nazarov, D. Thierry, Application of Scanning Kelvin Probe in the Study of Protective Paints, *Frontiers in Materials* 6 (2019), art. 192
- [21] M. Stratman, H. Streckel, R. Feser, A new technique able to measure directly the delamination of organic polymer films, *Corrosion Science* 32 (1991), 467-470
- [22] W. Fürbeth, M. Stratman, The delamination of polymeric coatings from electrogalvanized steel – a mechanistic approach. Part 3: delamination kinetics and influence of CO₂, *Corrosion Science* 43 (2001), 207-227
- [23] A. Amirudin, D. Thierry, Application of electrochemical impedance spectroscopy to study the degradation of polymer-coated metals, *Progress in Organic Coatings* 26 (1995), 1-28
- [24] J.N. Murray, Electrochemical test methods for evaluating organic coatings on metals: an update. Part III: Multiple test parameter measurements, *Progress in Organic Coatings* 31 (1997), 375-391

-
- [25] P.L. Bonora, F. Deflorian, L.Fedrizzi, Electrochemical impedance spectroscopy as a tool for investigating underpaint corrosion, *Electrochimica Acta* 41 (1996), 1073-1082
- [26] K. Ogle, S. Morel, N. Meddahi, An electrochemical study of the delamination of polymer coatings on galvanized steel, *Corrosion Science* 47 (2005) 2034-2052
- [27] F. Deflorian, S. Rossi, *An EIS study of ion diffusion through organic coatings*, *Electrochimica Acta* 51 (2006), 1736-1744
- [28] E. Akbarinezhad, M. Bahremandi, H.R. Faridi, F. Rezaei, Another approach for ranking and evaluating organic paint coatings via electrochemical impedance spectroscopy, *Corrosion Science* 51 (2009), 356-363
- [29] J-B. Jorcin, E. Aragon, N. Pébère, Delaminated areas beneath organic coating: A local electrochemical impedance approach, *Corrosion Science* 48 (2006) 1779-1790
- [30] V. Shkirskiy, A. Krasnova, T. Sanchez, A. Amar, V. Vivier, P. Volovitch, *Development of anodic and cathodic blisters at a model Zn/epoxy interface studied using local electrochemical impedance*, *Electrochemistry Communications* 111 (2020), 106633
- [31] J.J. Santana, J. González-Guzmán, J. Izquierdo, S. González, R.M. Souto, Sensing electrochemical activity in polymer-coated metals during the early stages of coating degradation by means of the scanning vibrating electrode technique, *Corrosion Science* 52 (2010), 3924-3931
- [32] V. Shkirskiy, P. Volovitch, V. Vivier, Development of quantitative Local Electrochemical Impedance Mapping: an efficient tool for the evaluation of delamination kinetics, *Electrochimica Acta* 235 (2017) 442-452
- [33] K.N. Allahar, G.P. Bierwagen, V.J. Gelling, *Understanding ac-dc-ac accelerated test results*, *Corrosion Science* 52 (2010), 1106-1114
- [34] J.J. Suay, M.T. Rodríguez, R. Izquierdo, A.H. Kudama, J.J. Saura, *Rapid assessment of automotive epoxy primers by electrochemical techniques*, *Journal of Coatings Technology* 75 (2003), 103-111
- [35] M. Bethencourt, F.J. Botana, M.J. Cano, R.M. Osuna, M. Marcos, *Lifetime prediction of waterborne acrylic paints with the AC-DC-AC method*, *Progress in Organic Coatings* 49 (2004), 275-281
- [36] J. Hollaender, Rapid assessment of food/package interactions by electrochemical impedance spectroscopy (EIS), *Food Additives and Contaminants* 14 (1997), 617-626
- [37] R. Montoya, F.R. García-Galván, A. Jiménez-Morales, J.C. Galván, *A cathodic delamination study of coatings with and without mechanical defects*, *Corrosion Science* 82 (2014), 432-436
- [38] H. Leidheiser, *Cathodic delamination of polybutadiene from steel: a review*, *Journal of Adhesion Science Technology* 1 (1987) 79-98
- [39] J. Zhang, G. S. Frankel, Corrosion-Sensing Behavior of an Acrylic-Based Coating System, *CORROSION* 55 (1999), 957-967
- [40] F. Maia, J. Tedim, A.C. Bastos, M.G.S. Ferreira and M.L. Zheludkevich, *Active sensing coating for early detection of corrosion processes*, *RSC Advances* 34 (2014), 17780-17786
- [41] G. Howarth, The use of water-based epoxies for anti-corrosive primers, *Anti-Corrosion Methods and Materials* 43 (1996), 23-28
- [42] T.H.Y. Qhach, Etude de la durabilité d'un primaire epoxy anticorrosion: rôle de l'interphase polymère/métal et conséquence sur l'adhérence, PhD Manuscript (2010), Polymères. Université du Sud Toulon Var, fftel-00647580
- [43] W. Fürbeth, M. Stratman, The delamination of polymeric coatings from electrogalvanized steel – a mechanistic approach. Part 1: delamination from a defect with intact zinc layer
- [44] D. Iqbal, R. Singh Moirangthem, A. Bashir, A. Erbe, Study of polymer coating delamination kinetics on zinc modified with zinc oxide of different morphologies, *Materials and Corrosion* 65 (2014), 370-375
- [45] S.K. Mallapragada, N.A. Peppas, Dissolution mechanism of semicrystalline poly(vinyl alcohol) in water, *Polymer Physics* 34 (1996), 1339-1346
- [46] A. Nazarov, N. Le Bozek, D. Thierry, Assessment of steel corrosion and deadhesion of epoxy barrier paint by scanning Kelvin probe, *Progress in Organic Coatings* 114 (2018), 123-134
- [47] J.T. Zhang, J.M. Hu, J.Q. Zhang, C.N. Cao, Studies of water transport behavior and impedance models of epoxy-coated metals in NaCl solution by EIS, *Progress in Organic Coatings* 51 (2004), 141-151
- [48] M.G. Olivier, M. Poelman, Use of Electrochemical Impedance Spectroscopy (EIS) for the evaluation of Electrocoatings performances, *Recent researches in corrosion evaluation and protection Chapter 1*, Intech (2012)
- [49] X. Gu et al., Linking Accelerated Laboratory Test with Outdoor Performance Results for a Model Epoxy Coating System, *Service Life Prediction of Polymeric Materials* (2009) Springer, 3-28

-
- [50] A.C. Rouw, Model epoxy powder coatings and their adhesion to steel, *Progress in Organic Coating* 34 (1988), 181-192
- [51] D. Nguyen Dang, S. Cohendoz, S. Mallarino, S. Touzain, *Effects of curing program on mechanical behavior and water absorption of DGEBA/TETA epoxy network*, *Journal of applied polymer science* 129 (2013), 2451-2463
- [52] J. R. Moraes d'Almeida, G. Wagner de Menezes, S. Neves Monteiro, *Ageing of the DGEBA/TETA Epoxy System with off-Stoichiometric Compositions*, Vol. 6, No. 3, (2003)
- [53] A.L. Bernassau, D. Hutson, C.E.M. Demore, S. Cochran, *Characterization of an Epoxy Filler for Piezocomposites Compatible with Microfabrication Processes*, *IEEE Transactions on Ultrasonic, Ferroelectrics, And Frequency Control* 58 (2011), 2743-2748
- [54] A. Charlesby, Crosslinking and degradation of polymers. *Radiation Physics and Chemistry* (1977) 18, 59
- [55] S. Morsch, S. Lyon, S.R. Gibbon, *The degradation mechanism of an epoxy-phenolic can coating*, *Progress in Organic Coatings*, 6th International Conference: Advances in Corrosion Protection by Organic Coatings 102, Part A, 37-43
- [56] S. Morsch, S. Lyon, P. Greensmith, S.D. Smith, S.R. Gibbon, *Water transport in an epoxy-phenolic coating*. *Progress in Organic Coatings* 78 (2015), 293-299
- [57] P. Musto, L. Mascia, G. Ragosta, G. Scarinzi, P. Villano, The transport of water in a tetrafunctional epoxy resin by near-infrared Fourier transform spectroscopy, *Polymer* 41 (2000), 565-574
- [58] J. Hollaender, R. Brandsch, *Application of impedance methods for corrosion protecting properties of coated substrates in metal packaging*, *International Meeting on Corrosion Science and Control Technologies, IMCORR, Rio de Janeiro, Brazil* (1995).
- [59] D.S. Viera, P.R.G. Fernandes, H. Mukai, R.S. Zola, G.G. Lenzi, E.K. Lenzi, Surface roughness influence on CPE parameters in electrolytic cells, *International Journal of Electrochemical Science* 11 (2016), 7775-7784
- [60] D. Gervasio, I. Song, J.H. Payer, *Determination of the oxygen reduction products on ASTM A516 steel during cathodic protection*, *Journal of Applied Electrochemistry*, 28 (1998), 972-989
- [61] H. Leidheiser, W. Wang, Some Substrate and Environmental Influences on the Cathodic Delamination of Organic Coatings, *Journal of Coatings Technologies* 53 (1981), 77
- [62] F. Zhou, D. Thierry, *Localized electrochemical impedance spectroscopy for studying the degradation of organic coatings*, *Electrochimica Acta* 42 (1997), 3293-3301
- [63] G. Williams, and H.N. McMurray, *The mechanism of group (I) chloride initiated filiform corrosion on iron*, *Electrochemical Communications* 5 (2003), 871-877
- [64] V. Upadhyay, D. Battocchi, *Localized electrochemical characterization of organic coatings: A brief review*, *Progress in Organic Coatings* 99 (2016), 365-377
- [65] S.R. Taylor, *Incentives for using local electrochemical impedance methods in the investigation of organic coatings*, *Progress in Organic Coatings* 43 (2001), 141-148
- [66] K. Darowicki, M. Szociński, A. Zieliński, Assessment of organic coating degradation via local impedance imaging, *Electrochimica Acta* 55 (2010), 3741-3748

Figure captions

Fig. 1. Schematic representation of **(a)** chemical bonding in cured DGEBA-TETA epoxy resin (adapted from Bernassau *et al.* [53]) and **(b)** epoxy degradation induced by interfacial pH increase.

Fig. 2. Schematic description of the AC-DC-AC procedure cycle used in the study.

Fig. 3. ATR-IR spectra (a, b) and evolution of peaks intensities with time (c, d) of the epoxy polymer over Zn HDG in the low wavelength region. **(a)** after 100 h of immersion and **(b)** after 7 AC-DC-AC cycles compared with the initial spectra of as coated epoxy polymer as indicated; **(c)** average evolution of the OH peaks intensities corresponding to “free -OH” and “total -OH” as a function of immersion time (see text for definition) and **(d)** average evolution of epoxy characteristic peaks (Table 1) intensities as a function of immersion time. Dashed line in **(c)** corresponds to the exponential fitting with Eq. 3 of the peaks intensities (A) vs immersion time (t).

Fig. 4. Evolution of average contact angle values on the model epoxy surface **(a)** in humid atmosphere (over 95%) and immersion in 10 mM NaCl water as indicated, **(b)** in modified AC-DC-AC ageing test.

Fig. 5. Examples of optical images of the epoxy coating on Zn after **(a)** 50 h; **(b)** 60; **(d)** 70 and **(e)** 75 h of immersion in a 10 mM NaCl electrolyte by *in situ* Time Lapse Microscopy. Images **(c)** and **(d)** represent 3D image composition in initial state (10 h of immersion) and after 75 h of immersion consequently. Strong deformation after immersion can be seen (see text for details).

Fig. 6. Typical EIS spectra **(a)** and evolution of average low frequency electrochemical impedance modulus **(b, c)** of model epoxy coated Zn at different immersion times (example after 1 and 72 h of immersion time) in a 10 mM NaCl aqueous solution. **(a, b)** during immersion and **(c)** under modified AC-DC-AC degradation procedure

Fig. 7. Typical EIS response of Zn alloy with two types of conversion coatings (Type 1 and Type 2 substrates in Tab. 1) in a 10 mM NaCl solution over modified AC-DC-AC aging procedure for **(a)** uncoated substrates and **(b, c)** substrates with model epoxy coating. Figure **(c)** presents average evolution of the low frequency electrochemical impedance modulus for the samples shown in (b).

Fig. 8. *In situ* Time Lapse Microscopy observation during OCP measurement after 3 and 5 AC-DC-AC test cycles for epoxy coated Zn alloy samples of type 1B and type 2B as indicated.

Fig. 9. *in situ* TLM **(a, c)** and LEIM maps **(b, d)** of the Zn alloy sample of type 1B (Type 1 substrate covered with model epoxy) after 4 AC-DC cycles **(a, b)** and type 1A (Type 1 substrate coated with strong epoxy primer) after 10 AC-DC cycle **(c, d)**. The areas mapped by LEIM are delimited in TLM images by squares.

Fig. 10. Schematic description of the metal/polymer interface degradation in the proposed accelerated test. During immersion, water and aggressive species diffuse through the polymer and reach the metal/polymer interface **(a)**. In function of weak **(b)** or strong **(c)** stability of the metal/oxide/polymer interface, the underpaint reactivity under polarization leads to different intensity of cathodic reaction and to different EIS response (Type 1 or Type 2) respectively. Finally, hydroxides generated at the interface diffuse through the coating and degrade the polymer **(d)**.

Tables

Table 1: Studied samples (substrate and polymer types, used name, number of studied samples N), applied degradation tests and characterizations methods.

Substrate		Polymer	Name	N	Degradation	Characterizations
Metal	Oxide					
Zn		model	Zn	10	Immersion	ATR-IR/EIS/TLM
		model	Zn	6	AC-DC-AC	ATR-IR/EIS/TLM
Zn alloy	Type 1 (defective)	thick	1A	2	Immersion, AC-DC-AC	Optical images
		model	1B	4		
	Type 2 (intact)	thick	2A	2	Immersion, AC-DC-AC	Optical images
		model	2B	4		

Table 2: Attribution of ATR-IR peak positions to characteristic groups of DGEBA-TETA epoxy resin

Peaks attribution	Wavelength / nm	Legend
OH-stretching ($\nu_1 + \nu_3$) characteristic of "total" water with hydrogen bonds	3400 (large)	1
ν C(sp ³)-H - alkanes	2924 - 2853.5	5
OH-bending (ν_2) characteristic of "free" OH in water	1644	6
δ -NH	1608.5	2
δ -NH (secondary amine)	1509	2
δ -C(sp ³)-H (alkanes in plain)	1460.5	5
CO in epoxides	1247	3
Trimethylol propane triglycidether cyclic ether	1182.5	
CO in aliphatic ethers	1108.5	4

Figure 1

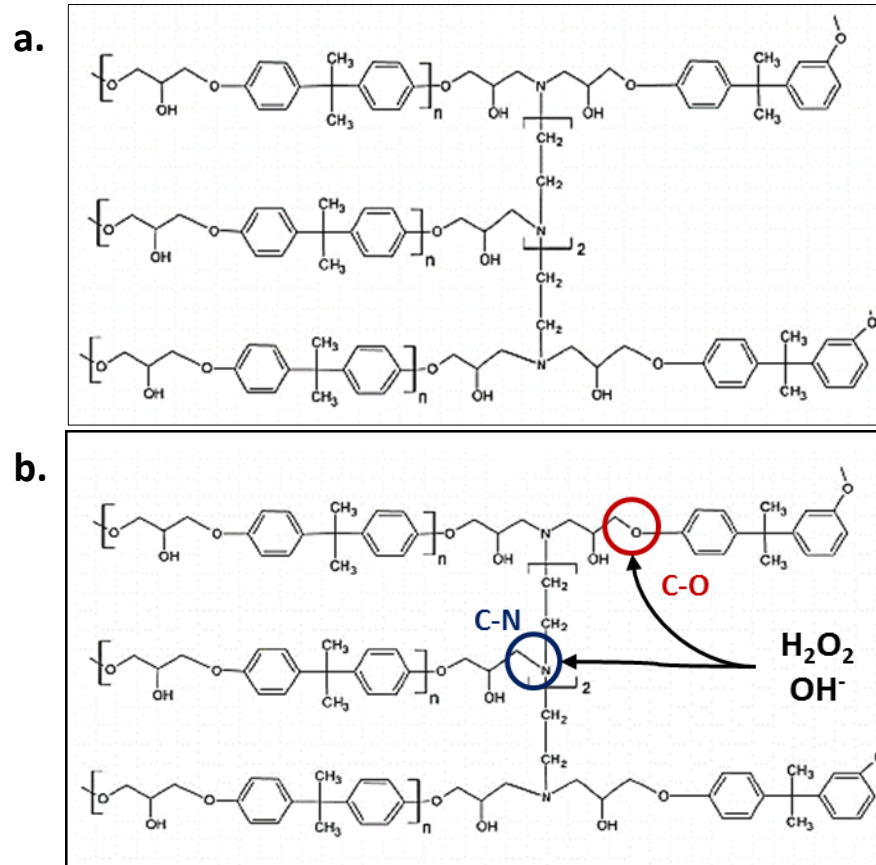


Figure 2

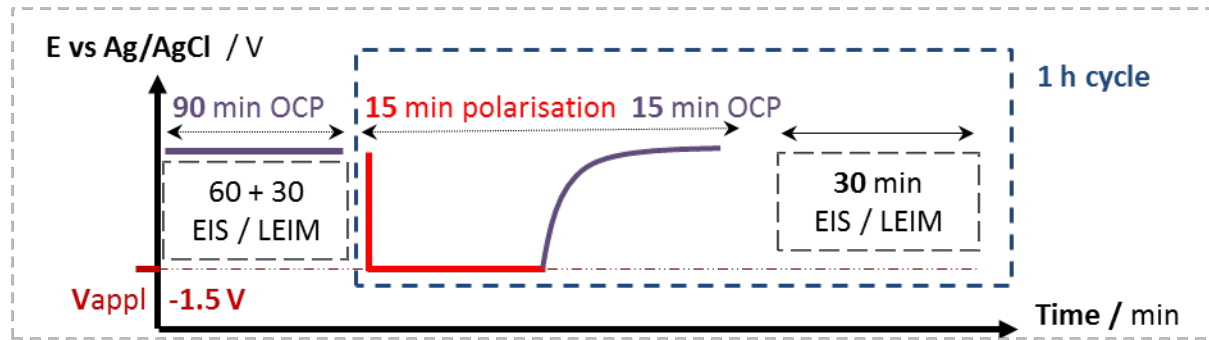


Figure 3

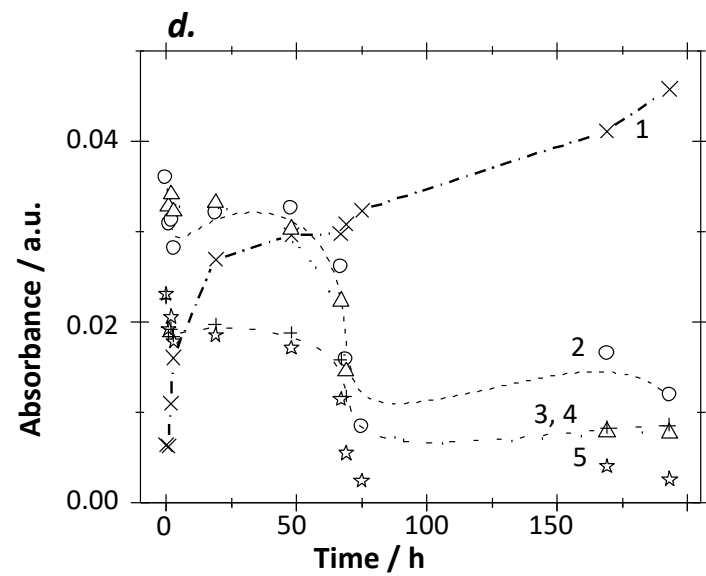
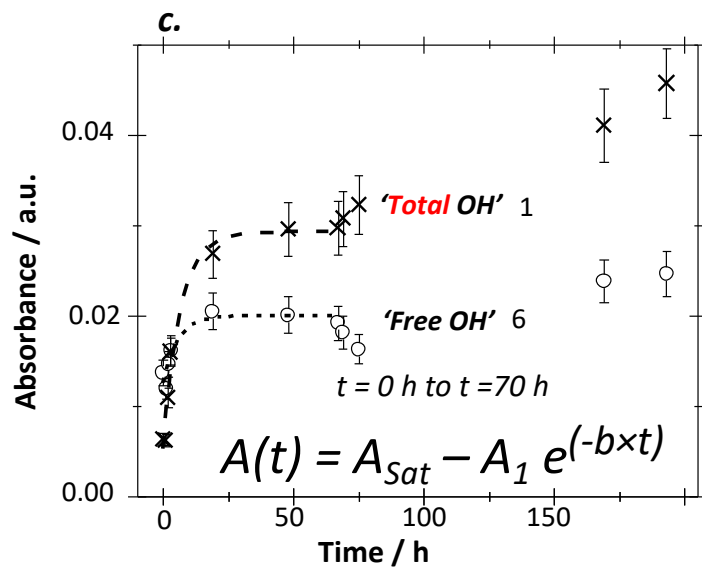
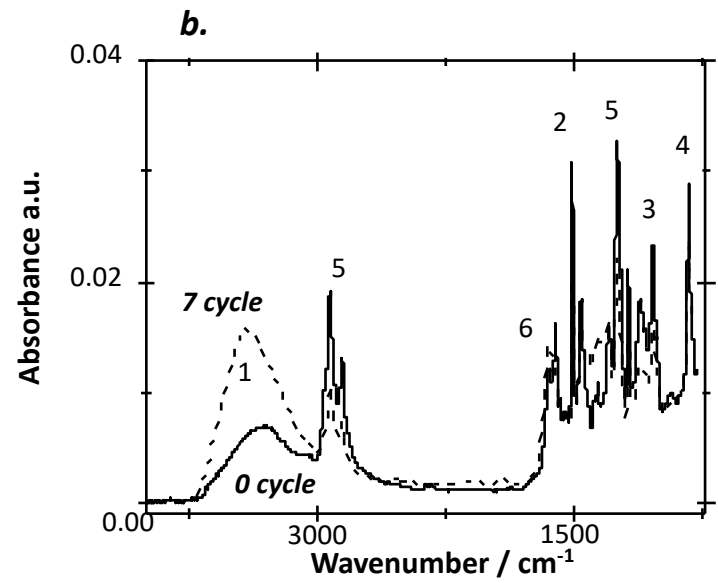
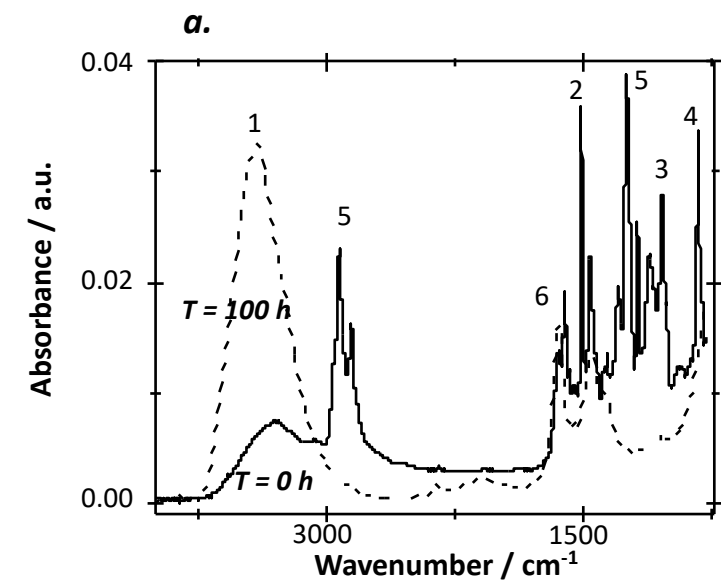


Figure 4

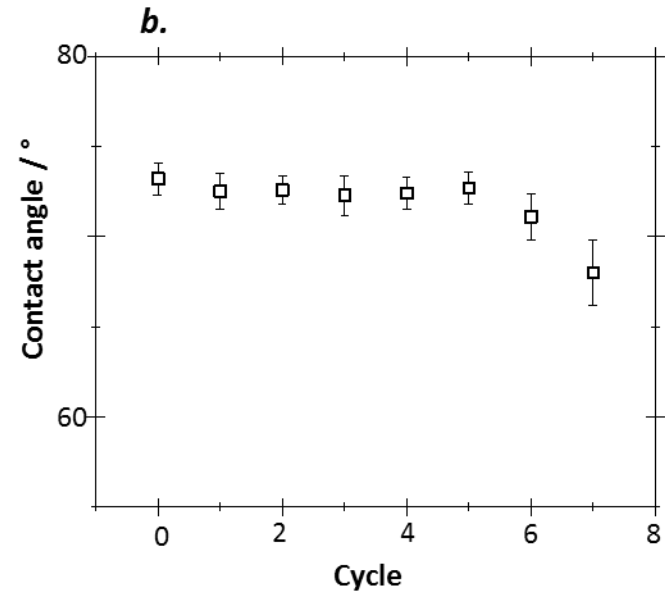
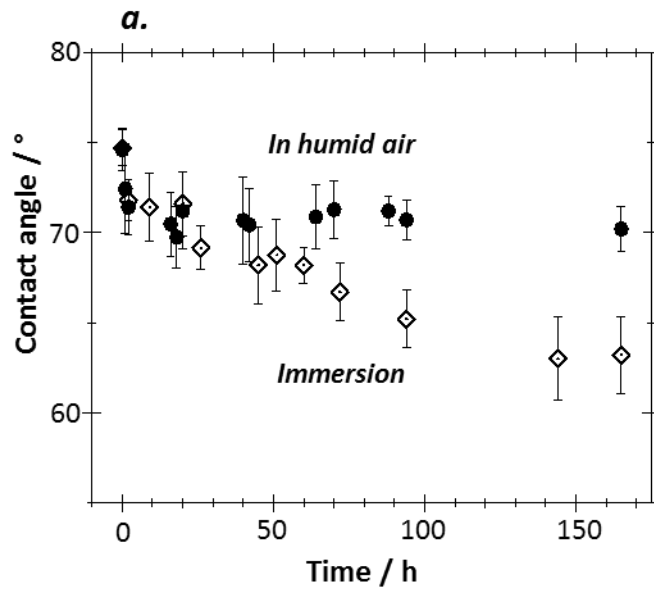
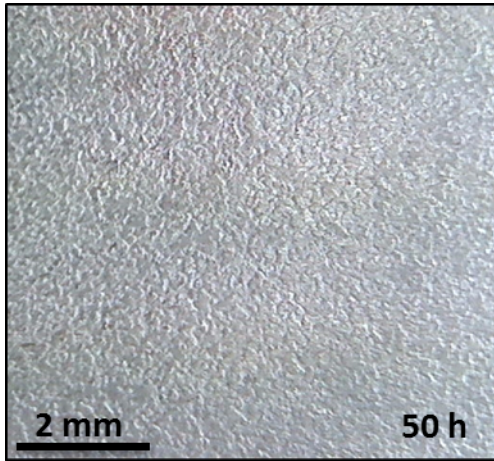
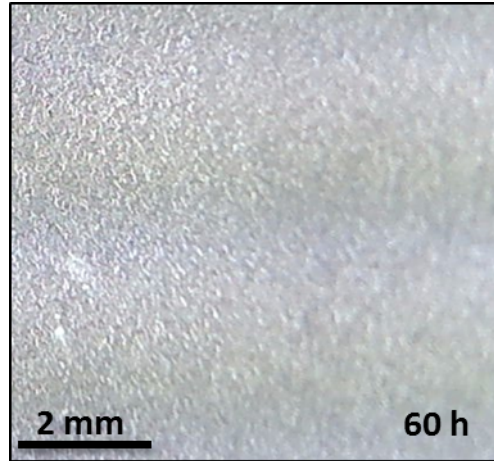


Figure 5

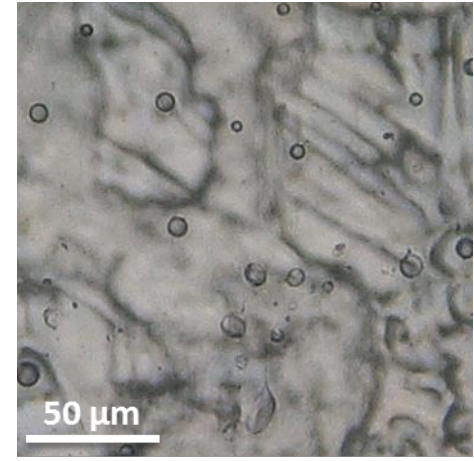
a.



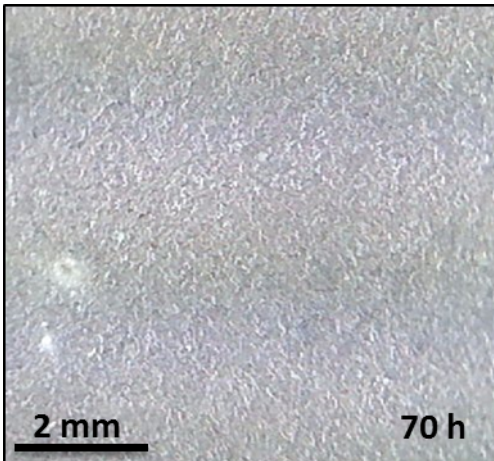
b.



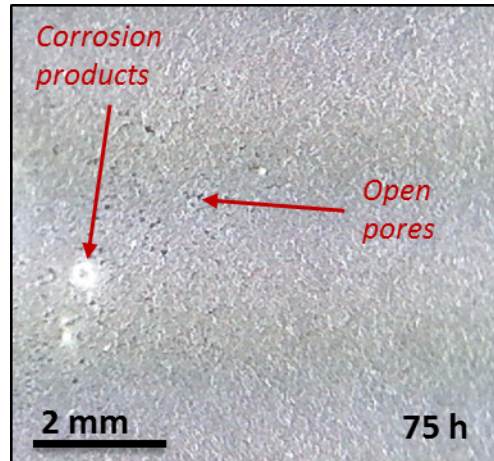
c.



d.



e.



f.

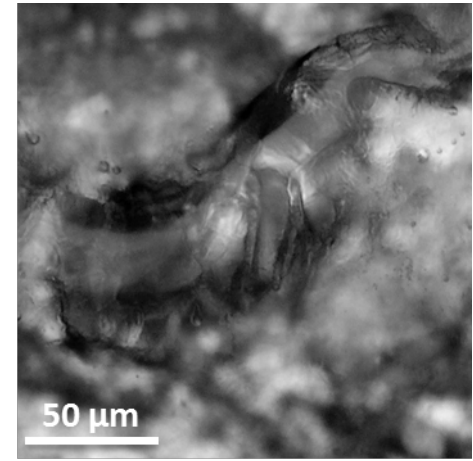


Figure 6

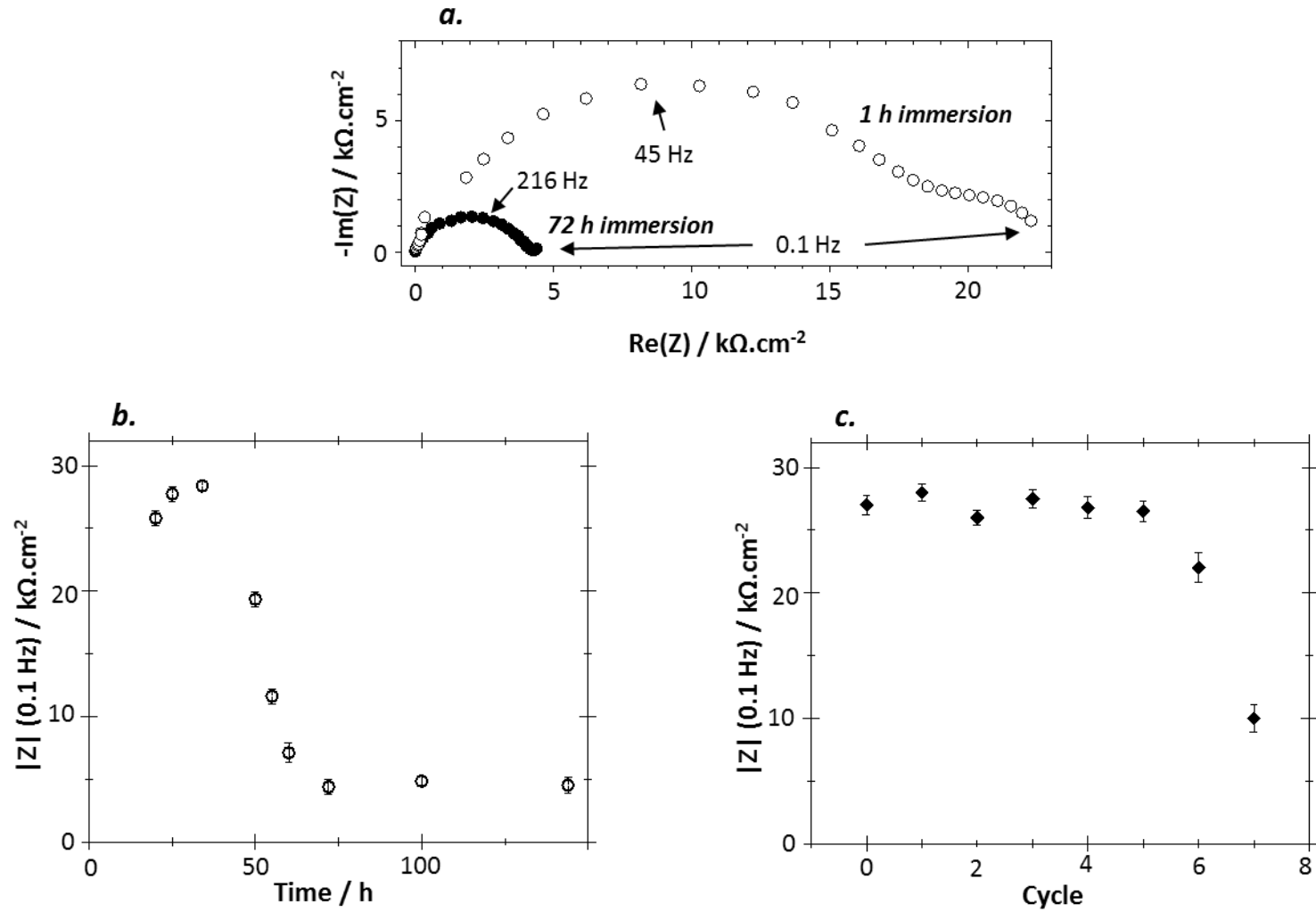


Figure 7

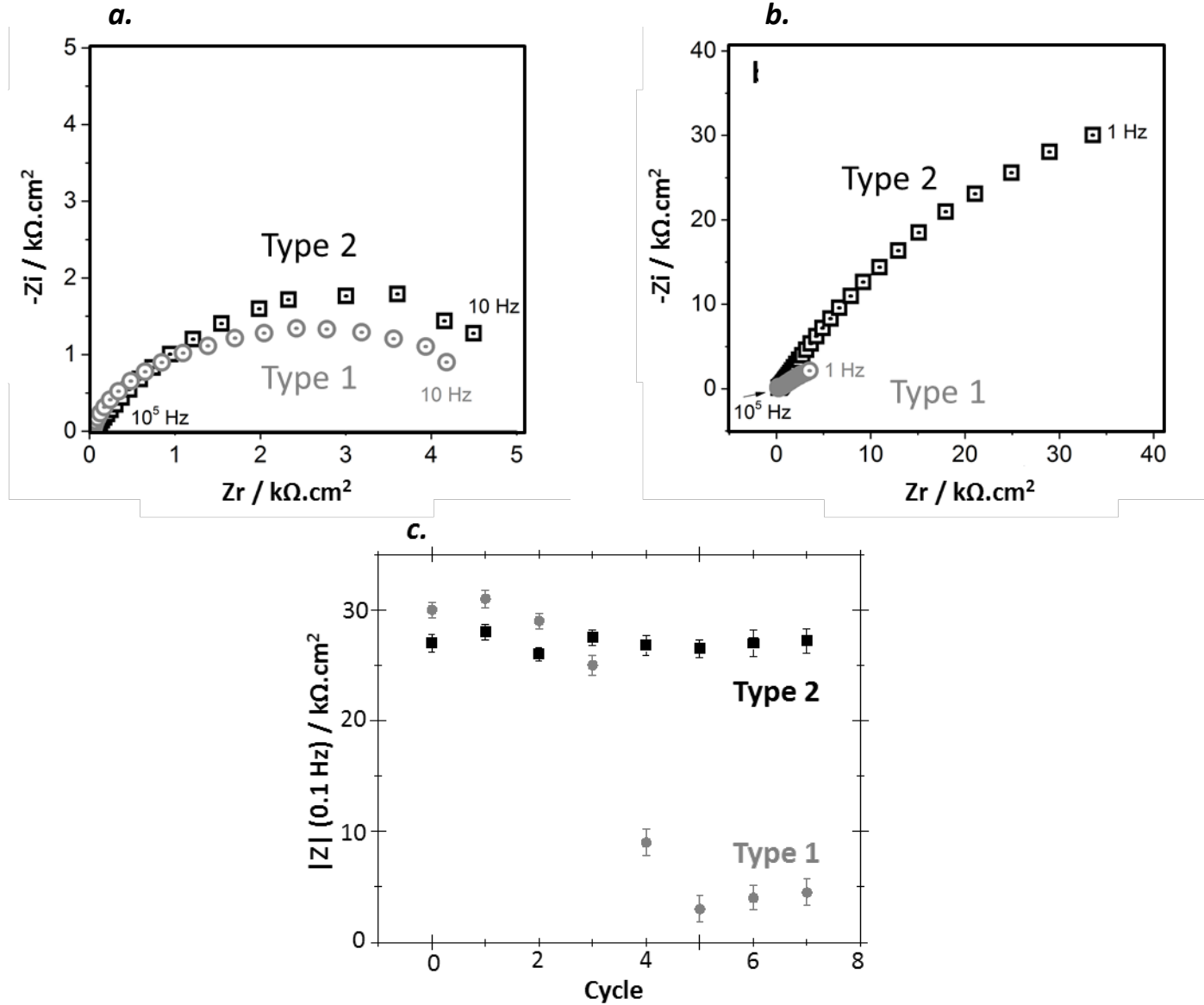


Figure 8

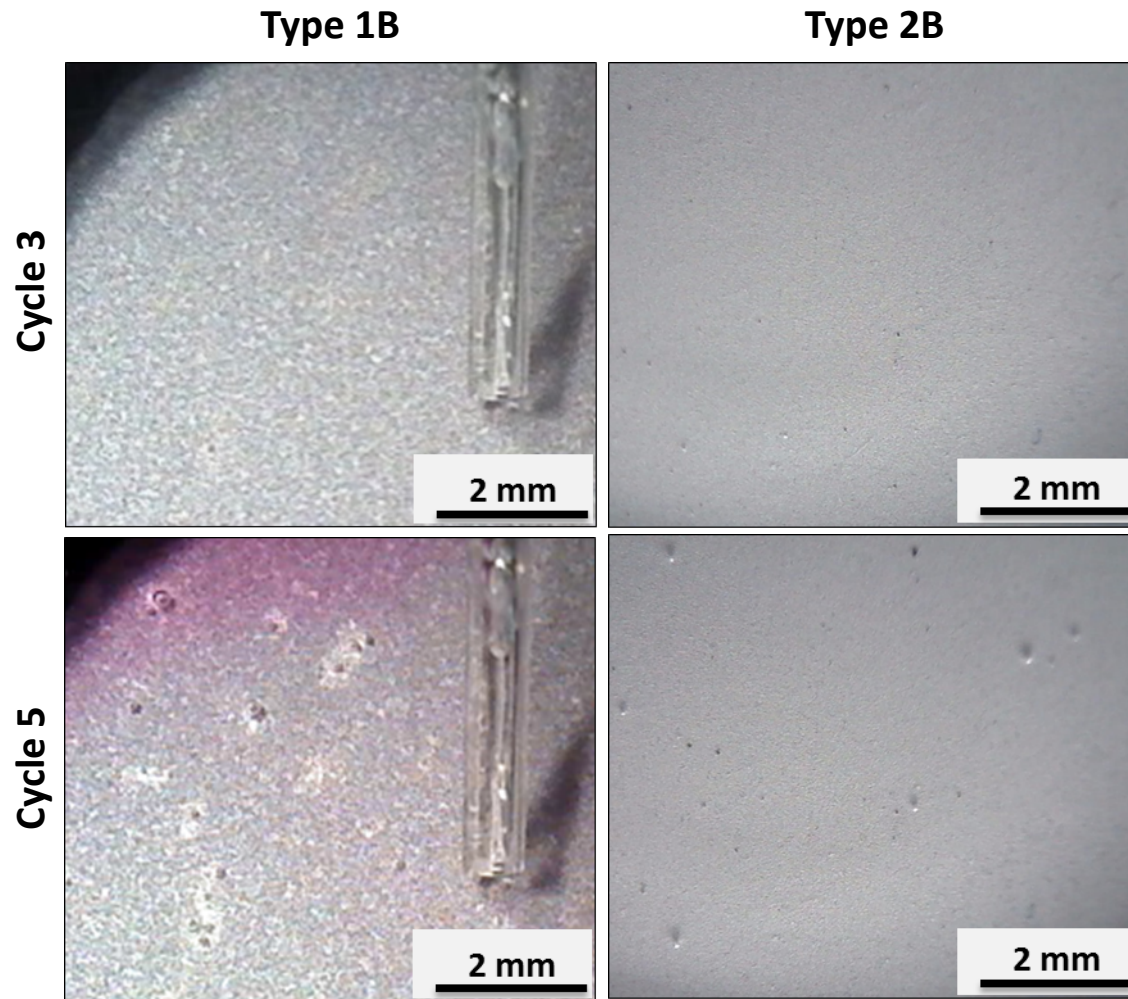


Figure 9

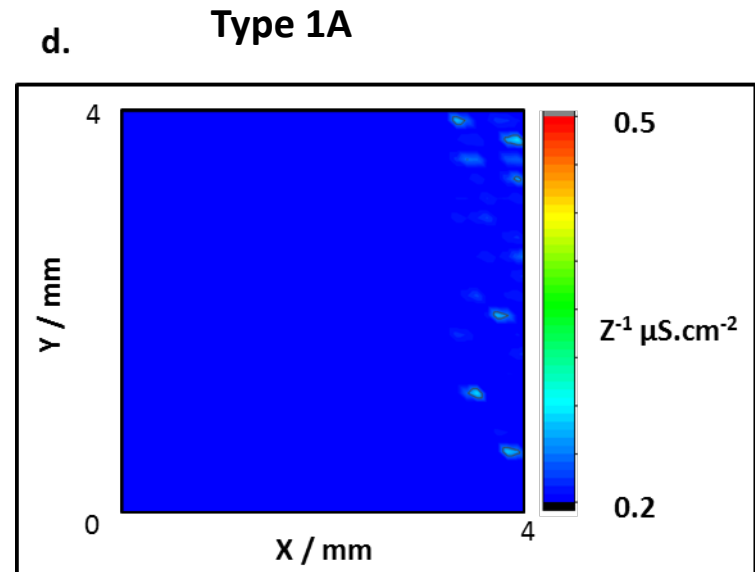
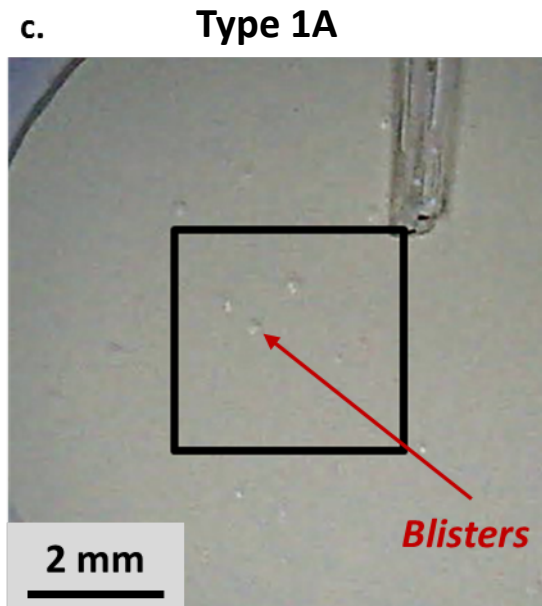
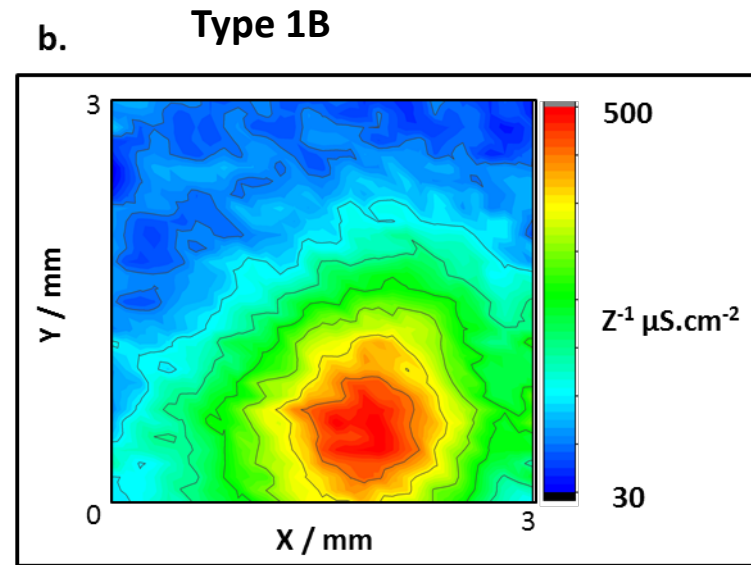
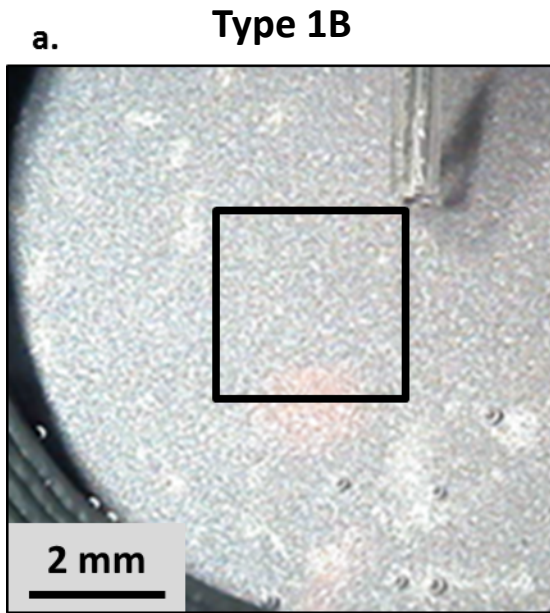


Figure 10

